Procatalytic Ligand Strain. Ionization and Perturbation of 8-Nitroxanthine at the Urate Oxidase Active Site†

Charles Doll,‡ Alasdair F. Bell,§ Nicholas Power,‡ Peter J. Tonge,§ and Peter A. Tipton*,‡

Department of Biochemistry, University of Missouri−Columbia, Columbia, Missouri 65211, and Department of Chemistry, Stony Brook University, Stony Brook, New York 11794-3400

Received April 28, 2005; Revised Manuscript Received July 7, 2005

ABSTRACT: The binding of the inhibitor 8-nitroxanthine to urate oxidase has been investigated by Raman and UV−visible absorption spectroscopy. The absorption maximum of 8-nitroxanthine shifts from 380 to 400 nm upon binding to the enzyme, demonstrating that the electronic structure of the ligand is perturbed. It has been proposed that oxidation of the substrate urate by urate oxidase is facilitated by formation of the substrate dianion at the enzyme active site, and Raman spectra of urate oxidase-bound 8-nitroxanthine suggest that both the dianionic and monoanionic forms of the ligand are bound to the enzyme under conditions where in solution the monoanion is present exclusively. The C4−C5 stretching frequency appears as a relatively isolated vibrational mode in 8-nitroxanthine whose frequency shifts according to the protonation state of the purine ring. Identification of the C4−C5 stretching mode was confirmed using [4-^{13}C]-8-nitroxanthine and ab initio calculation of the vibrational modes. Two peaks corresponding to the C4−C5 stretching mode were evident in spectra of enzyme-bound 8-nitroxanthine, at 1541 and 1486 cm^{-1}. The higher frequency peak was assigned to monoanionic 8-nitroxanthine, and the low-frequency peak was assigned to dianionic 8-nitroxanthine. The C4−C5 stretching frequency for free monoanionic 8-nitroxanthine was at 1545 cm^{-1}, indicating that the enzyme polarizes that bond when the ligand is bound. The C4−C5 stretching frequency in dianionic 8-nitroxanthine is also shifted by 4 cm^{-1} to lower frequency upon binding. For 8-nitroxanthine free in solution, the C4−C5 stretching frequency shifts to lower frequency upon deprotonation, and the absorption maximum in the UV−visible spectrum shifts to higher wavelength. The spectral shifts observed upon binding of 8-nitroxanthine to urate oxidase are consistent with increased anionic character of the ligand, which is expected to promote catalysis in the reaction with the natural substrate urate. In the Raman spectra of 8-nitroxanthine bound to the F179A, F179Y, and K9M mutant proteins, the C4−C5 stretching frequency was not perturbed from its position for the unbound ligand. Both V_{max} and V/K were decreased in the mutant enzymes, demonstrating a correlation between the interaction that perturbs the C4−C5 stretching frequency and the catalytic activity of the enzyme. It is suggested that hydrogen-bonding interactions that lead to precise positioning and deprotonation of the substrate are perturbed by the mutations.

Urate oxidase catalyzes the O_2-dependent oxidation of urate to form 5-hydroxyisourate. In contrast to most O_2-dependent enzymes urate oxidase does not utilize any cofactor, and the catalytic reaction appears to proceed by activation of the substrate undergoing oxidation, rather than by activation of O_2. Transient-state kinetics and trapping experiments have identified urate hydroperoxide as an intermediate in the reaction (*1*, *2*). Urate hydroperoxide is believed to form from O_2 and the urate dianion. Steady-state kinetic studies have provided evidence for a general base whose role is to generate the dianion from the urate monoanion that binds to the active site (*3*, *4*). Oxidation of the urate dianion is extremely facile, and computational studies have revealed that the regiochemistry of the oxidation predicted from the distribution of electrons in the dianion is consistent with the structure of the hydroperoxide intermediate and the product (*5*). Collapse of the hydroperoxide and subsequent hydration of the dehydrourate intermediate lead to the generation of the observed product (Scheme 1). Thus, what appears to be a complicated reaction for the enzyme to catalyze, is, in many ways, reduced to the much simpler task of generating the dianion of urate in the presence of O_2.

Recent studies have demonstrated that enzyme active sites can generate forces to polarize or distort substrates in ways that promote catalysis. For example, Raman spectroscopy studies of serine proteases have demonstrated that the polarization of the carbonyl of the acyl-enzyme intermediate correlates well with k_{cat} (*6*). Similarly, polarization of the carbonyl on the substrate of 4-chlorobenzoyl-coenzyme A

† This project was supported by the National Research Initiative of the USDA Cooperative State Research, Education and Extension Service, Grant 2002-35318-12519 to P.A.T., and by Grant GM63121 from the National Institutes of Health to P.J.T. In addition, this material is based upon work supported in part by the U.S. Army Research Office under Grant DAAG55-97-1-0083 to P.J.T. P.J.T. is an Alfred P. Sloan Fellow.

* To whom correspondence should be addressed. Telephone: (573) 882-7968. Fax: (573) 884-4812. E-mail: tiptonp@missouri.edu.

‡ University of Missouri.

§ Stony Brook University.

10.1021/bi0507837 CCC: $30.25 © 2005 American Chemical Society
Published on Web 08/06/2005

Scheme 1

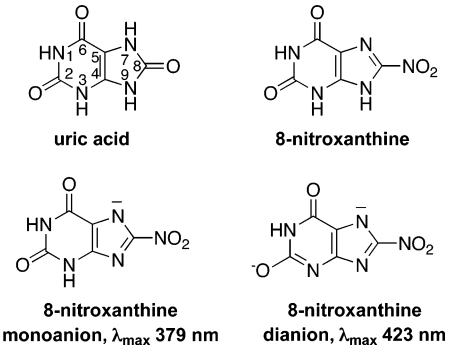

dehalogenase correlated with rates of formation of the intermediate Meisenheimer complex (*7*). NMR and Raman studies revealed that cinnamoyl-coenzyme A substrates become polarized at the active site of enoyl-CoA hydratase, and the strain energy that was imposed was estimated to be >3 kcal/mol (*8*).

Mechanisms for accelerating the rate of the urate oxidase reaction could include facilitating formation of the urate dianion and providing complementarity to the transition state for urate hydroperoxide formation. In addition to an appropriately positioned general base, the active site could provide residues that modulate the electron density of the substrate through hydrogen bonds. Since urate is planar and urate hydroperoxide is not, the enzyme could also impose geometrical distortions on the substrate that would be expected to facilitate catalysis.

To investigate whether ligands are structurally perturbed upon binding at the active site of urate oxidase in a manner that would facilitate catalysis, we have employed Raman and UV-visible absorption spectroscopy to characterize binding of 8-nitroxanthine. 8-Nitroxanthine (Scheme 1) is a competitive inhibitor versus urate ($K_i = 2.1 \pm 0.1$ μM at pH 8.0) and a convenient spectroscopic probe, because the electron-withdrawing nitro group causes a bathochromic shift in the absorption maximum relative to unsubstituted purines, so interference by protein absorption and scattering is minimized. The results suggest that binding to the urate oxidase active site does induce procatalytic changes in the electronic structure of the ligand; that is, if those forces were imposed on urate, they would facilitate its oxidation by increasing its anionic character. Significantly, a fraction of the population of bound 8-nitroxanthine appears to be in the dianionic form.

MATERIALS AND METHODS

Recombinant urate oxidase from *Bacillus subtilis* was expressed and purified from *Escherichia coli*, as described previously (*4*). Site-directed mutants were constructed with the Quik-Change mutagenesis kit (Strategene) following the manufacturer's protocol. All potential mutants were sequenced at the University of Missouri DNA Core to verify the incorporation of the mutation and the integrity of the rest of the gene. Wild-type and mutant urate oxidase proteins were assayed by monitoring H_2O_2 production (*4*). Assays were conducted in air-saturated 50 mM Tris, pH 8.0; urate solutions were prepared fresh before each use.

Synthesis of 8-Nitroxanthine. 8-Nitroxanthine was synthesized by nitration of xanthine (*9*). [4-^{13}C]Xanthine was prepared as follows. [4-^{13}C]Diaminouracil (100 mg, 0.42 mmol), prepared according to Bentley and Neuberger (*10*), was intimately mixed with potassium formate (116 mg, 1.38 mmol). The mixture was placed in a round-bottom flask equipped with a magnetic stir bar and heated to 220 °C under an inert atmosphere for 30 min. After being cooled to room temperature the contents of the flask were dissolved in a minimal amount of ammonium hydroxide, aided by gentle warming. Red, insoluble material was removed by filtration. The filtrate was triturated with glacial acetic acid, until a precipitate formed at pH 4−5. The precipitate was collected by filtration and washed with cold H_2O and methanol. ^{13}C NMR (DMSO-d_6): δ 152.4 (C-2), δ 149.8 (C-4), δ 107.8 (C-5), δ 156.5 (C-6), δ 141.5 (C-8).

[4-^{13}C]-8-Nitroxanthine was obtained as follows. [4-^{13}C]-Xanthine (73 mg, 0.46 mmol) was placed in a round-bottom flask and dissolved in 0.5 mL of glacial acetic acid containing HNO_3 (160 mg, 2.3 mmol). The solution was refluxed at 120 °C under N_2 for 5 h. The solution was cooled to room temperature, and the yellow crystals that formed were collected by filtration. The filtrate was reserved, and additional product precipitated out over time. The crystals were washed with cold H_2O and methanol and dried under vacuum. The crude product was recrystallized from 20 mL of 0.5 M HCl. UV−visible absorption spectrum (H_2O): λ_{max} 380 nm. ^{13}C NMR (DMSO-d_6): δ 151.1 (C-2), δ 145.7 (C-4), δ 111.3 (C-5), δ 156.2 (C-6), δ 146.8 (C-8).

8-[^{15}N]Nitroxanthine was prepared as described above for the ^{13}C-labeled 8-nitroxanthine, using $H^{15}NO_3$ in the nitration. The labeled nitric acid was prepared by mixing $K^{15}NO_3$ (2 g, 19.6 mmol) with H_2SO_4 (3.16 mL, 59 mmol) in a 15 mL round-bottom flask. The reaction mixture was distilled under vacuum at 45−60 °C, and the distillate was trapped in a coldfinger immersed in liquid N_2.

UV−Visible Spectroscopy. Absorption spectra of 8-nitroxanthine bound to urate oxidase were obtained with a Cary 50 spectrophotometer; difference spectra were obtained by subtracting the spectrum of urate oxidase from that of the urate oxidase−8-nitroxanthine complex. Samples were buffered in 50 mM Tris, pH 8.0, and contained 50 μM urate oxidase active sites and 10 μM 8-nitroxanthine.

Raman Spectroscopy. The Raman spectra were acquired with 500 mW of 752 nm laser excitation using an instrument described in detail elsewhere (*11*). The Raman measurements were made by adding 70 μL of protein (180 μM in 50 mM Tris, pH 8.0) to a 2 mm by 2 mm quartz cuvette and collecting data for 10 min. Subsequently, between 1 and 2 μL of concentrated 8-nitroxanthine stock solution was added to the same cuvette and a second spectrum recorded. The difference spectra were then calculated by subtracting the spectrum of protein alone from that of the protein plus ligand using a small correction factor to account for the dilution of the protein sample upon addition of ligand. All of the Raman data were calibrated against cyclohexanone, and the data are accurate to ± 1 cm^{-1}. Data acquisition was performed with WinSpec software (Princeton Instruments), and spectra were processed using Win-IR. Under the conditions used for acquiring good quality difference data on proteins the resolution of our system was 8 cm^{-1}.

Computational Studies. Vibrational spectra for the fully protonated, monoanionic, and dianionic forms of 8-nitroxanthine were calculated using the Gaussian 98 or Gaussian 03 suite of programs (*12*). 8-Nitroxanthine deprotonates

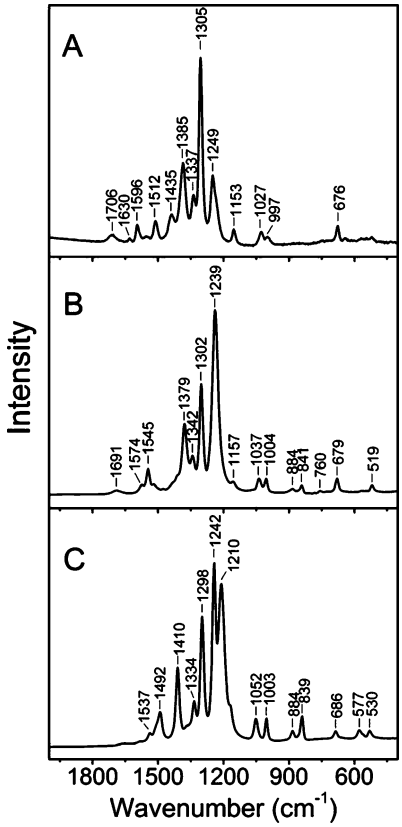

FIGURE 1: Raman spectra of 8-nitroxanthine. (A) Neutral 8-nitroxanthine in 0.1 M HCl. (B) Monoanionic 8-nitroxanthine at pH 8.0. (C) Dianionic 8-nitroxanthine in 0.1 M NaOH.

sequentially from the N7, N3, and N1 positions (*9*), so calculations were performed for the N7-deprotonated monoanion and the N3,N7-deprotonated dianion. Calculations were performed with the B3LYP functional and the 6-31+G(d,p) basis set. Each structure was minimized, and then vibrational modes were calculated for the minimized structures. The calculated frequencies were corrected by multiplying by a factor of 0.9614.

RESULTS

Raman Spectroscopy. Raman spectra of 8-nitroxanthine in the neutral, monoanionic, and dianionic states are shown in Figure 1. Neutral 8-nitroxanthine has 45 vibrational modes, and the monoanion and dianion have 42 and 39 vibrational modes, respectively. Many of these fall outside of the experimental spectral window; between 400 and 2000 cm^{-1} approximately one-half to two-thirds of the possible vibrational modes were observed. Some of the peaks were assigned on the basis of experimentally observed shifts in 8-[^{15}N]nitroxanthine and [4-^{13}C]-8-nitroxanthine. Modes that involved substantial proton motion were evident from spectra obtained in D_2O (data not shown). Other peaks were assigned by comparison to calculated values. Table 1 lists the observed Raman peaks and their tentative assignments for the 8-nitroxanthine monoanion. The spectra are dominated by peaks in the 1200−1300 cm^{-1} range, which arise from complex ring motions.

Although many of the observed peaks arise from coupled motions involving several atoms, each spectrum contained a peak that primarily reflects the C4−C5 stretching frequency. This peak appeared at 1596 cm^{-1} in neutral 8-nitroxanthine, at 1546 cm^{-1} in the monoanion, and at 1492 cm^{-1} in the dianion (Figure 1). Assignment of this peak was confirmed by substitution of ^{13}C at C4; the peak shifted to lower frequency by 38 cm^{-1} in neutral 8-nitroxanthine and by 25 cm^{-1} in the monoanion and the dianion. The magnitude of the shift upon isotopic substitution is consistent with the expected value for C=C stretching using a simple reduced mass calculation. The ab initio calculations for [4-^{13}C]-8-nitroxanthine predicted shifts of 25 cm^{-1} for neutral nitroxanthine, 23 cm^{-1} for the monoanion, and 18 cm^{-1} for the dianion.

Table 1: Assignments for the Raman Spectrum of 8-Nitroxanthine at pH 8.0

mode	frequency (cm^{-1})	assignment[a]
11 or 13	518	in-plane ring bending
17	679	in-plane ring stretching
23	842	$-NO_2$ scissor
24	885	N1−C2−N3 scissor
25	1005	N7−C8−N9 scissor
26	1038	symmetric N1H, N3H wag
	1157	?
28	1239	C6−C5−N7 symmetric stretch; NH3 wag
30	1302	$-NO_2$ symmetric stretch
31	1343	asymmetric NH1, NH3 wag
32	1378	N1−C2−N3 asymmetric stretch
36	1545	C4−C5 stretch
37	1574	$-NO_2$ asymmetric stretch
38	1687	N3−C4−N9 asymmetric stretch

[a] Assignments are based on B3LYP calculations with the 6-31+G(d,p) basis set, as described in the text. Although most modes involved motion of multiple atoms, only the dominant motions are listed. The output for the frequency calculations is provided in the Supporting Information and gives a complete description of the atomic motions for each vibrational mode.

Comparison of the spectra of 8-nitroxanthine in different protonation states reveals a number of small differences. Of particular interest are low-frequency peaks that appear at 577 and 530 cm^{-1} in the dianion. The spectrum of the monoanion shows only one of these peaks, appearing at 519 cm^{-1}, and the spectrum of neutral 8-nitroxanthine is featureless in this region. These features do not shift upon isotopic substitution with ^{13}C at C4 and ^{15}N in the nitro group or upon deuteration, suggesting that they arise from modes that are delocalized over many atoms. The calculated vibrational modes indicate that these peaks are likely to arise from in-plane bending modes that involve all of the atoms in the purine nucleus. Regardless of the specific origin of the low-frequency features, one can use them as a marker for the ionization state of 8-nitroxanthine.

The nitro group scissoring mode appears at 841 cm^{-1} in the 8-nitroxanthine monoanion. Assignment was confirmed by isotopic substitution; in 8-[^{15}N]nitroxanthine the peak shifted to 836 cm^{-1}. The calculated shift upon isotopic substitution was 5 cm^{-1}. In the 8-nitroxanthine dianion the nitro group scissoring mode appears at 839 cm^{-1}, and its relative intensity is much greater than the corresponding mode in the monoanion. The calculated intensity of the peak arising from the scissoring mode for the dianion is 20 times greater than that for the monoanion.

Similarly, the mode giving rise to a peak at 1003 cm^{-1} in the dianion is much more intense than the corresponding peak appearing at 1004 cm^{-1} in the monoanion. The position of

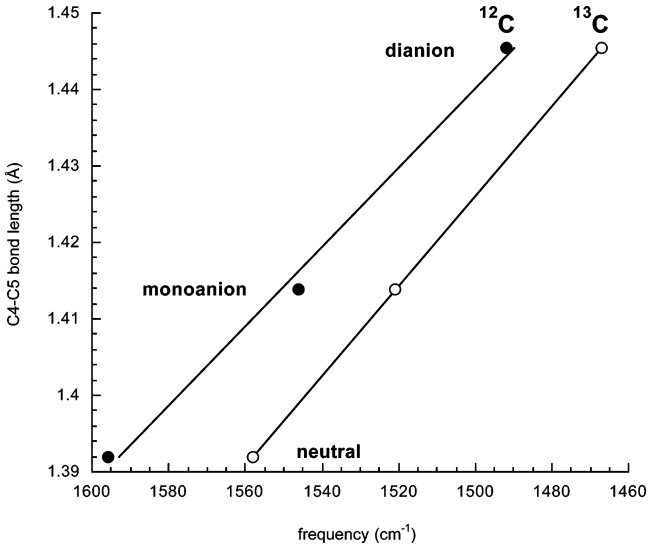

FIGURE 2: Correlation between measured frequency of the C4−C5 stretching mode in 8-nitroxanthine and the calculated C4−C5 bond length.

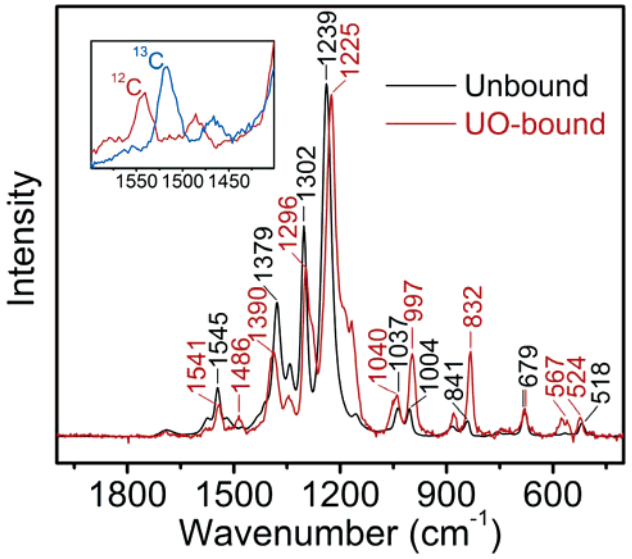

FIGURE 3: Raman spectra of 8-nitroxanthine at pH 8.0 free in solution (purple) and bound to urate oxidase (red). Inset: C4−C5 stretching region of enzyme-bound 8-nitroxanthine: unlabeled (red); [4-^{13}C]-8-nitroxanthine (blue).

this peak is invariant with isotopic substitution and relatively insensitive to the presence of D_2O. Calculations suggest that the peak arises from motions involving symmetrical stretching of the N7−C8−N9 bonds and asymmetric stretching of the C6−N1−C2 bonds in the dianion, and symmetrical stretching of the N7−C8−N9 bonds and symmetrical stretching of the N1−C2−N3 bonds in the monoanion.

Figure 3 shows the difference spectrum for 8-nitroxanthine bound to urate oxidase. The peak assigned to the C4−C5 stretching frequency of the monoanion at 1545 cm^{-1} is shifted to lower frequency by 4 cm^{-1}. Two peaks are present in the spectrum of enzyme-bound ligand that are absent in the spectrum of the 8-nitroxanthine monoanion. One peak appears at 1486 cm^{-1}, close to where the C4−C5 stretching frequency appears in the unbound 8-nitroxanthine dianion (1492 cm^{-1}). The inset to Figure 3 shows that both peaks assigned to the C4−C5 stretching frequency shift upon substitution of ^{13}C at C4. Thus both the 1541 and 1486 cm^{-1}

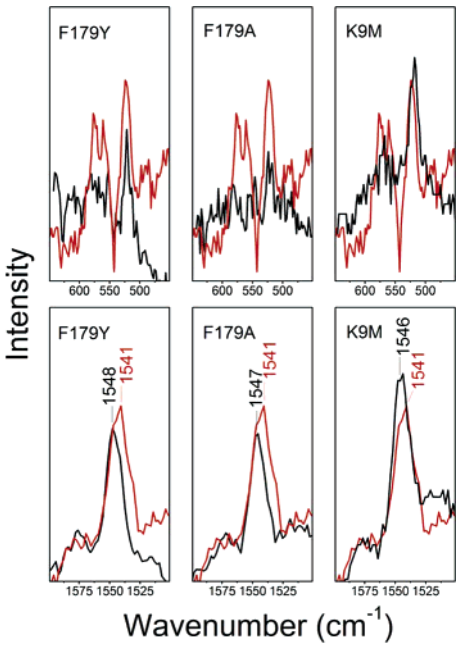

FIGURE 4: Raman spectra of 8-nitroxanthine bound to mutant urate oxidases. In each case, the spectrum obtained with the mutant protein is shown as the black line and is superimposed over the corresponding region of the wild-type protein, shown as a red line.

bands can be assigned to the C4−C-5 stretching frequency of monoanionic and dianionic 8-nitroxanthine bound to urate oxidase. For both anionic forms of the ligand, binding causes a small but significant (4−6 cm^{-1}) decrease in the frequency of the ν_{C4-C5} mode.

The presence of two bound ligand populations is also supported by further observations which indicate the presence of the 8-nitroxanthine dianion in the enzyme−ligand complex. The spectrum of the enzyme-bound ligand has a broad peak, which may arise from two unresolved peaks, centered at ~570 cm^{-1}. In the spectra of 8-nitroxanthine in the absence of protein, this peak appears only in the dianionic species. In addition, the relative intensity of the peak arising from the nitro group scissoring mode is enhanced in enzyme-bound 8-nitroxanthine, consistent with the normal mode calculations that predict a 20-fold increase in the Raman intensity of this mode upon deprotonation of the monoanion. Finally, the peak that appears at 1003 cm^{-1} in the 8-nitroxanthine monoanion shifts to 997 cm^{-1} when the ligand binds to urate oxidase, and its relative intensity increases. Again, normal mode calculations indicate that the intensity of this mode is larger for the dianion compared to the monoanion.

Several mutants of urate oxidase were also characterized with respect to 8-nitroxanthine binding. Phe179 is stacked below the planar ligand at the urate oxidase active site, and Lys9 has been proposed to function as part of a catalytic diad to deprotonate the substrate (*4*). The K9M, F179Y, and F179A mutants were prepared, and Figure 4 shows the peak arising from the C4−C5 stretch, and the low-frequency region that contains the peak that is diagnostic for the presence of the dianion, in each mutant. It is apparent that the shift to lower frequency in the C4−C5 stretch is not present in the mutants. Additionally, the peak at 570 cm^{-1} that seems to be a signature for the dianion is not observed in the mutant protein−ligand complexes.

The UV−visible difference spectra of 8-nitroxanthine bound to urate oxidase and the F179Y and F179A mutants

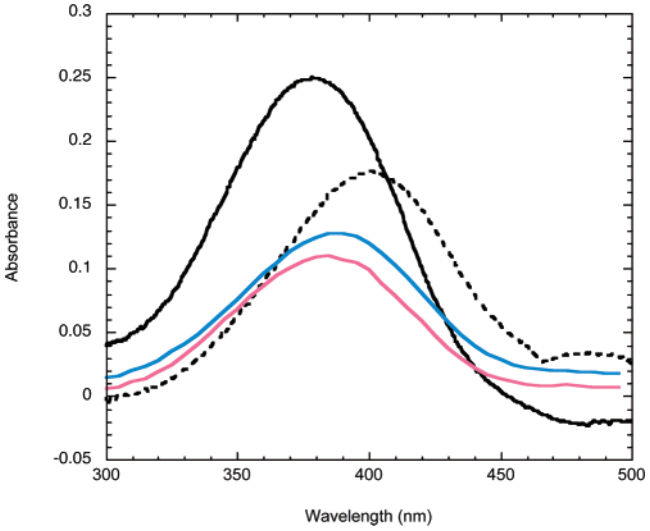

FIGURE 5: UV−visible spectrum of 8-nitroxanthine at pH 8.0 free in solution (black solid line) and bound to wild-type urate oxidase (black dashed line), F179A (blue solid line), and F179Y (red solid line).

Table 2: Steady-State Kinetic Parameters for Urate Oxidase and Site-Directed Mutants

enzyme	V_{max} (s^{-1})	K_m (μM)[a]	V/K ($\mu M^{-1}\,s^{-1}$)	K_d[b] (μM)
wild type	3.26 ± 0.12[b]	34 ± 5[b]	0.097 ± 0.015[c]	2.1 ± 0.1
F179Y	1.56 ± 0.04	64 ± 5	0.024 ± 0.004	4.4 ± 0.2
F179A	0.020 ± 0.001	28 ± 4	0.007 ± 0.002	11 ± 1
K9M	0.0135 ± 0.003	51 ± 8	0.0003 ± 0.0001	4.06 ± 0.02

[a] Apparent K_m for urate in air-saturated buffer. [b] Dissociation constant for 8-nitroxanthine. [c] Data taken from ref *4*.

are shown in Figure 5. In the absence of protein, the absorption maximum for the 8-nitroxanthine monoanion appears at 379 nm. Upon binding to urate oxidase, the maximum shifts to 399 nm. When 8-nitroxanthine is bound to the F179A mutant or the K9M mutant (data not shown), the absorption maximum is at 390 nm; the absorption maximum of the F179Y mutant is at 385 nm.

The steady-state kinetic parameters for the wild-type and mutant urate oxidases are given in Table 2. The dissociation constant for 8-nitroxanthine from each protein was determined by fluorescence titration, and the data are also presented in Table 2. The conservative mutation F179Y decreases V_{max} by 2-fold. Removal of the aromatic ring in the F179A mutant has a more dramatic effect, decreasing V_{max} by 2 orders of magniturde. Similarly, the K9M mutant, which should not be able to generate the dianion of urate, is decreased in activity by over 200-fold.

DISCUSSION

Urate oxidase catalyzes the reaction between urate and molecular oxygen to form a hydroperoxide intermediate. Since no cofactors participate in the catalytic cycle, it appears that the enzyme activates urate for reaction, in contrast to many O_2-dependent enzymes, which activate O_2 for reaction with the substrate undergoing oxidation. We sought to determine whether we could detect any procatalytic perturbations, that is, forces that the enzyme placed on a ligand bound at the active site, that would enhance the oxidation of urate if they were imposed on it in an analogous manner.

The pH dependence of nonenzymatic urate oxidation shows that the reaction is much more facile with the dianion than with the monoanion, which in turn oxidizes more easily than the neutral species (*13*). Computational studies revealed that the adiabatic ionization potential decreases with successive deprotonations of uric acid (*5*). Clearly, generation of the urate dianion at the active site is one way to facilitate the oxidation of urate, and the enzyme can utilize general base catalysis for proton abstraction. Other mechanisms for achieving rate acceleration can be envisioned as well. The product of O_2 addition is the C5 urate hydroperoxide; since C5 is sp^2-hybridized in the substrate and sp^3-hybridized in the product, any force that the enzyme imposed on the substrate to deform it away from planarity would be expected to enhance oxidation.

As uric acid is deprotonated, electron density accumulates at C5, which conveniently explains the regiochemistry of the oxidation, and the C4−C5 bond lengthens from 1.366 to 1.409 Å (*5*). The C4−C5 bond length is calculated to be 1.540 Å in urate hydroperoxide. Thus, polarization and elongation of the C4−C5 bond is indicative of changes in electronic structure that facilitate oxidation. Deprotonation of the urate monoanion is clearly procatalytic, but it may also be considered to represent one extreme of a continuum of changes in electronic structure that the enzyme could impose on the substrate. Absorption and vibrational spectroscopy are sensitive methods to detect subtle changes in electronic structure.

The absorption maximum of 8-nitroxanthine at pH 8.0 is 379 nm; the p*K*'s for 8-nitroxanthine are 2.12 and 9.84 (*9*), so at pH 8 it is almost exclusively monoanionic. Upon binding to urate oxidase at pH 8.0, the absorption maximum shifts to 399 nm; the absorption maximum for dianionic 8-nitroxanthine is 423 nm (*9*), so the shift upon binding to the enzyme is consistent with the ligand gaining dianionic character, or ionization of a fraction of the population of enzyme-bound ligands.

To gain more detailed information about the changes in the electronic structure of 8-nitroxanthine that occurred upon binding, we turned to Raman spectroscopy. Changes in the character of the C4−C5 bond should appear in the Raman spectra; specifically, perturbations that result in an increase in the C4−C5 bond length should result in a shift of the peak arising from the stretching motion to lower frequency. This expectation was borne out by model studies characterizing neutral 8-nitroxanthine, the monoanion, and the dianion. As shown in Figure 2, a good linear correlation exists between the experimentally determined frequency of the peak arising from C4−C5 stretching and the C4−C5 bond length calculated by density functional methods. The assignment of the peak to the C4−C5 stretch was substantiated by computational studies and substitution of ^{13}C at the C4 position. When 8-nitroxanthine is bound to urate oxidase at neutral pH, the peak arising from the C4−C5 stretching motion is shifted to lower frequency by 4 cm^{-1}. On the basis of the correlation shown in Figure 2, this frequency shift represents a perturbation approximately 15% of the way to the full dianion. Although this is a relatively small effect, it is consistent with the notion that binding at the active site involves protein−ligand interactions that are procatalytic. The magnitude of the shift that is observed in the present work is similar to that observed in studies of enoyl-CoA hydratase,

in which the enzyme imposed perturbations on the ligand at the active site that caused changes in the ligand vibrational spectrum that were equivalent to approximately 10% of the change along the reaction coordinate that would be required to reach the transition state (*14*).

Unexpectedly, the spectra of enzyme-bound 8-nitroxanthine also showed peaks assignable to another species which appears to be the dianion. The Raman spectra of 8-nitroxanthine in different ionization states suggest that the peak at 570 cm^{-1}, which is unique to the dianion, may serve as a signature for its presence. As is evident from Figure 3, one distinct difference between enzyme-bound 8-nitroxanthine and free ligand at pH 8.0 is the presence of a peak at 570 cm^{-1} in spectra of the enzyme-bound ligand that is absent in spectra of the free ligand.

The peak at 1480 cm^{-1} is in the region of the spectrum where the C4−C5 stretch occurs in the enzyme-free dianion. The peak shifts by 22 cm^{-1} to lower frequency upon substitution with ^{13}C at C4, consistent with the assignment to a C═C stretching mode. This vibrational mode appears at even lower frequency than the C4−C5 stretch in the 8-nitroxanthine dianion, which appears at 1492 cm^{-1}, suggesting that the C4−C5 bond in the bound ligand has even more single bond character than the free dianion. Several mechanisms could be employed to deplete electron density in the C4−C5 bond of the enzyme-bound ligand. Hydrogen bond donation to the ligand could withdraw electron density from the C4−C5 bond. Geometrical deformation of the ligand away from planarity would shift C5 more toward sp^3 hybridization, which would also decrease electron density in the C4−C5 bond. It is noteworthy that calculations indicate that the most stable conformer of the urate dianion is nonplanar (*5*); B3LYP/6-31+G(d,p) calculations indicate that the angle between the pyrimidine ring and the imidazole ring is 175.9° (data not shown). If the enzyme provided a binding pocket in which optimal interactions could be achieved only with nonplanar ligands, the effect would be to facilitate catalysis.

In summary, the spectroscopic data demonstrate that the enzyme generates the dianion of 8-nitroxanthine at the active site and imposes forces that perturb the electronic structures of the monoanion and dianion. These perturbations are manifested in a decrease in ν_{C4-C5}, which indicates that the C4−C5 bond lengthens. This suggests that the forces in place at the active site do not simply lower the p*K* of the bound ligand. If that were the case, one would not expect to see ν_{C4-C5} perturbed in the dianion. Rather, it appears that the forces are able to delocalize electrons from the C4−C5 bond, regardless of the ionization state of the ligand. However, the fact that the dianion is present on the enzyme when the pH of the bulk solution dictates that it is present in negligible amounts in solution indicates that the enzyme does also lower the p*K* of the second ionizable group. Geometric distortion of the ligand and modulation of the p*K*'s of its ionizable groups are certainly interrelated; however, they are not necessarily synonymous. For example, one could imagine electrostatic or hydrogen bond interactions with the purine nitrogens that would change their p*K*'s but would not effect the planarity of the molecule. Both effects observed here, decreasing the p*K* of the second ionizable group and decreasing the electron density in the C4−C5 bond, when applied to the substrate urate, should be procatalytic. If one accepts the view that the critical step in the urate oxidase reaction is the formation of the dianion, then it is clear that any mechanism that facilitates the deprotonation of the monoanion should facilitate catalysis. Likewise, since the urate dianion is nonplanar and peroxide formation occurs at C5, forces that increase electron density at C5 at the expense of the C4−C5 bond will be procatalytic.

Three site-directed mutants of urate oxidase were characterized with respect to 8-nitroxanthine binding to determine if the perturbations that were observed upon binding to wild-type enzyme could be assigned to interactions with individual amino acid residues. Site-directed mutagenesis and pH kinetic studies have provided evidence that urate oxidase employs general base catalysis to generate the dianionic substrate at the active site (*3*, *4*). K9 is believed to deprotonate T69, which then deprotonates the substrate. Unfortunately, the role of T69 in inducing structural perturbations in 8-nitroxanthine could not be probed, because mutagenesis at that position resulted in weak ligand binding. However, the K9M mutant still bound 8-nitroxanthine tightly and had significantly reduced catalytic activity. Urate oxidase also has a conserved phenylalanine residue at the active site (F179 in *B. subtilis* urate oxidase); the conservative F179Y mutation results in a 2-fold decrease in V_{max}, while the F179A mutation causes a decrease in V_{max} of 2 orders of magnitude.

None of the three mutant proteins showed the perturbations to 8-nitroxanthine that were observed with the wild-type enzyme. The peak assigned to the C4−C5 stretching mode did not shift to lower frequency, and the peak at 570 cm^{-1} that appears to be a signature for the presence of the dianion was absent. Furthermore, the peak at 1486 cm^{-1} observed with the wild-type protein and assigned to the 8-nitroxanthine dianion C4−C5 stretching mode was absent in spectra obtained with the mutant proteins. These data strengthen the suggestion that K9 is involved in deprotonation of the ligand and suggest that F179 also plays a role in generating or stabilizing the dianion, although it is not obvious what that role may be. The correlation between disappearance of the spectral signatures for the 8-nitroxanthine dianion and loss of activity is not perfect, in that the spectrum obtained with the F179Y mutant is lacking those features, but its activity is only reduced 2-fold relative to the wild-type enzyme. This may reflect subtle differences in the ways urate and 8-nitroxanthine interact with urate oxidase.

A small but growing number of enzymes that utilize oxygen without the benefit of a cofactor are being recognized. Recent work suggests that the cofactor-independent dioxygenase 1*H*-3-hydroxy-4-oxoquinaldine 2,4-dioxygenase catalyzes the formation of the dianion of its substrate prior to reaction with oxygen to generate a hydroperoxide intermediate (*15*). The chemical advantage of dianion formation is clear; increased negative charge on the substrate facilitates its oxidation. Following formation of the dianion, electron transfer to molecular oxygen creates a radical pair as the first step in the sequence of events that must occur in order to overcome the spin-forbidden nature of the reaction between oxygen and a spin-paired organic substrate. Like urate oxidase, 1*H*-3-hydroxy-4-oxoquinaldine 2,4-dioxygenase catalyzes the oxidation of a substrate that can form a radical anion with relative ease. Although the cofactor-independent oxidases and oxygenases are not related to one another in any evolutionary sense, the chemical imperative

of each one's catalytic reaction suggests that dianion formation will be a common feature of their mechanisms (*15*). In the case of urate oxidase, it appears that binding at the active site leads to perturbations that promote formation of the dianion.

SUPPORTING INFORMATION AVAILABLE

The calculated vibrational modes for neutral, monoanionic, and dianionic 8-nitroxanthine and the corresponding 4-^{13}C-labeled isotopomers. This material is available free of charge via the Internet at http://pubs.acs.org.

REFERENCES

1. Kahn, K., and Tipton, P. A. (1998) Spectroscopic characterization of intermediates in the urate oxidase reaction, *Biochemistry 37*, 11651−11659.
2. Sarma, A. D., and Tipton, P. A. (2000) Evidence for urate hydroperoxide as an intermediate in the urate oxidase reaction, *J. Am. Chem. Soc. 122*, 11252−11253.
3. Kahn, K., and Tipton, P. A. (1997) Kinetic mechanism and cofactor content of soybean root nodule urate oxidase, *Biochemistry 36*, 4731−4738.
4. Imhoff, R. D., Power, N. P., Borrok, M. J., and Tipton, P. A. (2003) General base catalysis in the urate oxidase reaction: evidence for a novel Thr-Lys catalytic diad, *Biochemistry 42*, 4094−4100.
5. Kahn, K. (1999) Theoretical studies of intermediates in the urate oxidase reaction, *Bioorg. Chem. 27*, 351−362.
6. Tonge, P. J., and Carey, P. R. (1990) Length of the acyl carbonyl bond in acyl-serine proteases correlates with reactivity, *Biochemistry 29*, 10723−10727.
7. Clarkson, J., Tonge, P. J., Taylor, K. L., Dunaway-Mariano, D., and Carey, P. R. (1997) Raman study of the polarizing forces promoting catalysis in 4-chlorobenzoate-CoA dehalogenase, *Biochemistry 36*, 10192−10199.
8. D'Ordine, R. L., Pawlak, J., Bahnson, B. J., and Anderson, V. E. (2002) Polarization of cinnamoyl-CoA substrates bound to enoyl-CoA hydratase: correlation of (13)C NMR with quantum mechanical calculations and calculation of electronic strain energy, *Biochemistry 41*, 2630−2640.
9. Mosselhi, M. A., and Pfleiderer, W. (1993) Purines. XIV[1]. Synthesis and properties of 8-nitroxanthine and its *N*-methyl derivatives, *J. Heterocycl. Chem. 30*, 1221−1228.
10. Bentley, R., and Neuberger, A. (1952) The mechanism of action of uricase, *Biochem. J. 52*, 694−699.
11. Bell, A. F., He, X., Wachter, R. M., and Tonge, P. J. (2000) Probing the ground state structure of the green fluorescent protein chromophore using Raman spectroscopy, *Biochemistry 39*, 4423−4431.
12. Frisch, M. J., Trucks, G. W., Schlegel, H. B., Scuseria, G. E., Robb, M. A., Cheeseman, J. R., Montgomery, J. A., Jr., Vreven, T., Kudin, K. N., Burant, J. C., Millam, J. M., Iyengar, S. S., Tomasi, J., Barone, V., Mennucci, B., Cossi, M., Scalmani, G., Rega, N., Petersson, G. A., Nakatsuji, H., Hada, M., Ehara, M., Toyota, K., Fukuda, R., Hasegawa, J., Ishida, M., Nakajima, T., Honda, Y., Kitao, O., Nakai, H., Klene, M., Li, X., Knox, J. E., Hratchian, H. P., Cross, J. B., Adamo, C., Jaramillo, J., Gomperts, R., Stratmann, R. E., Yazyev, O., Austin, A. J., Cammi, R., Pomelli, C., Ochterski, J. W., Ayala, P. Y., Morokuma, K., Voth, G. A., Salvador, P., Dannenberg, J. J., Zakrzewski, V. G., Dapprich, S., Daniels, A. D., Strain, M. C., Farkas, O., Malick, D. K., Rabuck, A. D., Raghavachari, K., Foresman, J. B., Ortiz, J. V., Cui, Q., Baboul, A. G., Clifford, S., Cioslowski, J., Stefanov, B. B., Liu, G., Liashenko, A., Piskorz, P., Komaromi, I., Martin, R. L., Fox, D. J., Keith, T., Al-Laham, M. A., Peng, C. Y., Nanayakkara, A., Challacombe, M., Gill, P. M. W., Johnson, B., Chen, W., Wong, M. W., Gonzalez, C., and Pople, J. A. (2003) Gaussian, Inc., Pittsburgh, PA.
13. Goyal, R. N., Mittal, A., and Agarwal, D. (1994) Electrochemical oxidation and kinetics of the decay of UV-absorbing intermediate of uric acid oxidation at pyrolytic graphite electrodes, *Can. J. Chem. 72*, 1668−1674.
14. Bell, A. F., Feng, Y., Hofstein, H. A., Parikh, S., Wu., J., Rudolph, M. J., Kisker, C., Whitty, A., and Tonge, P. J. (2002) Stereoselectivity of enoyl-CoA hydratase results from preferential activation of one of two bound substrate conformers, *Chem. Biol. 9*, 1247−1255.
15. Frerichs-Deeken, U., Ranguelova, K., Kappl, R., Huttermann, J., and Fetzner, S. (2004) Dioxygenases without requirement for cofactors and their chemical model reaction: compulsory order ternary complex mechanism of 1*H*-3-hydroxy-4-oxoquinaldine 2,4-dioxygenase involving general base catalysis by histidine 251 and single-electron oxidation of the substrate dianion, *Biochemistry 43*, 14485−14499.

BI0507837